

First Experience with HERA Beams

U. Straumann, University of Zurich

1. Collider Status and Luminosity Measurement

HERA is a new collider, delivering luminosity to the users since June '92 at DESY in Hamburg. 26.7 GeV electrons collide with 820 GeV protons in two experimental areas, the south hall (experiment Zeus) and the north hall (experiment H1), thereby interacting at a center-of-mass energy of $\sqrt{s} = 300$ GeV. A complex layout of various accelerators including the old PETRA ring is used to feed electrons and protons into the new HERA tunnel (circumference 6.336 km). While the electron ring is equipped with conventional magnets, the proton ring's dipole and quadrupole magnets are superconducting.

To reach the planned peak luminosity of 10^{31} cm⁻²sec⁻¹, the rings will be filled with 210 bunches of electrons and protons respectively, leading to a bunch crossing interval of only 96 nsec, which represents a major challenge for the front end electronics and the trigger systems of the experiments.

During first operation this summer only 10 consecutive bunches were filled into the accelerator, the p (e) current per bunch being 7 (2) times smaller than the design value. With these conditions a luminosity of a few times 10^{28} cm⁻²sec⁻¹ could be reached, a value which is expected from scaling the design luminosity to the above mentioned conditions.

For the first time collisions involving leptons and hadrons were observed in a collider, and there were no space charge effects or other unforeseen difficulties. Typical luminosity runs lasted about four hours; the integrated luminosity, which was used for data-taking in the two experiments until the end of July, was about 1 nb⁻¹.

Both experiments have a special setup to measure the luminosity in their interaction region: the bremsstrahlung which the electron emits in the field of the proton is detected by a photon detector installed about 105 m upstream in the electron direction, while the electron is detected in a system located about 35 m upstream (numbers from H1). The acceptance

© U. Straumann 1993

for electrons (photons) is about $E_e = 6-16$ GeV ($E_\gamma = 10-20$ GeV). The rate of coincidences with the condition $E_e + E_\gamma = E_{\text{beam}}$ is a measure of the luminosity. To estimate backgrounds induced by electron-gas and electron-wall interactions, one of the bunches was filled with electrons only and did not collide with protons.

The lifetime of the proton beam is very long, sometimes staying more than one day in the accelerator. In contrast to this, at higher currents the electron beam shows a decay time of about two hours. This is still not understood completely. Therefore, rather frequently, the electron beam is dumped and immediately afterwards a new injection and acceleration of electrons allows use of the same proton beam for different luminosity periods.

In the near future there are plans to improve the technical reliability of various parts, specifically the power supplies of the system. The currents and number of bunches will increase stepwise to the design luminosity. About 50% transverse polarisation of the electron beam has already been observed.

2. The Physics Potential

Figure 2.1 specifies the kinematics of an ep event. Apart from the usual photon exchange propagator, the high center-of-mass energy gives rise to additional contributions due to the weak interaction propagators Z^0 and W^\pm , which allows the observation of charged current events at sufficiently high Q^2 .

The experiments are designed to measure the energy and direction of the target jet and the scattered electron (for neutral current events). The two basic Lorentz invariant quantities, x and Q^2 , are then over-determined by these four quantities, at least for neutral current events. This helps to reduce the measurement errors and allows basic cross checks of the measuring methods.

Figure 2.2 shows the regions for which the event kinematics are sufficiently well-determined that the systematic errors on the differential cross section are smaller than 20%. At high x there are limitations because the current jet is lost in the forward beampipe, while the large corrections due to final state electromagnetic radiation make the area close to $y = 1$ very difficult. If Q^2 is smaller than a few GeV^2 , the electron is

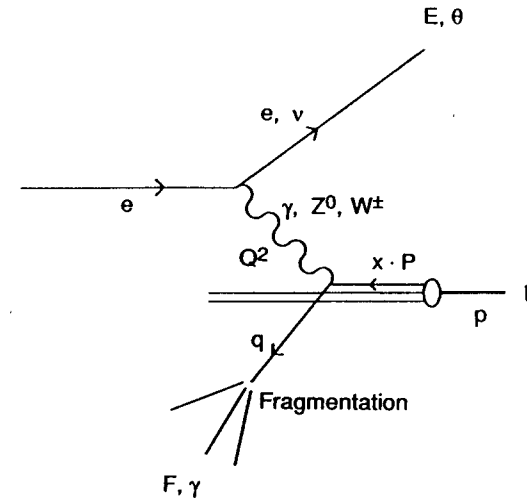


Figure 2.1: Basic kinematics of an ep event. The measured quantities are the energy of the scattered electron E and the total energy of the fragmented hadronic system F , the polar angle of the emitted electron θ and the average polar angle of the hadronic system γ . The Lorentz invariant quantities defining the event kinematics are Bjorken x (in the 'infinite momentum frame' the fraction of the proton momentum which is carried by the struck quark) and the 4-momentum transfer squared Q^2 . P denotes the momentum of the incoming proton.

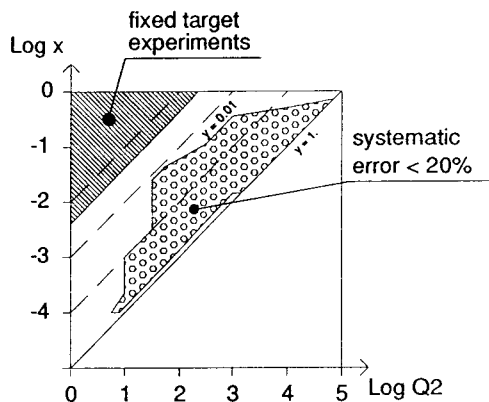


Figure 2.2: The region where the differential cross section for neutral current deep inelastic scattering can be measured with a systematic error of less than 20%. An explanation of the limits is given in the text. The region where fixed target data are presently available is also shown.

lost in the backward (proton side) beampipe, however the acceptance still reaches down to $x = 10^{-4}$.

These experiments probe the behaviour of the parton structure of the proton at Q^2 up to a few times 10^4 GeV^2 . Due to the effects of the Z propagator, the total parton momentum distributions can be measured by means of the structure function F_2 as in electron and muon beam fixed target experiments; quark and antiquark distributions can be distinguished by making use of the polarisation and different charges of the electron beam to determine xF_3 . At these very short space-time scales deviations from the expected behaviour of F_2 and xF_3 would possibly indicate new substructures of the quarks.

However, since the cross section scales with Q^{-4} a minimum integrated luminosity of at least 100 pb^{-1} is needed to come to any significant results; this corresponds to a measuring time of one year at full design luminosity. This discussion will therefore concentrate on the very low x and intermediate Q^2 region.

In this region the gluon density increases strongly with decreasing x , such that unitarity limits would be violated if there were not a saturation effect. Various models for these high gluon density distributions have been developed. In general, the theorists distinguish between three regions in the (x, Q^2) plane: at low gluon density there is a region where one believes perturbative QCD is well under control; at very high gluon densities the hadron looks fully packed with partons, and perturbation theory is certainly no longer applicable; in between there is a transition region, where perturbation theory is still usable but has to include additional effects from recombining gluons. Several authors also have discussed the possibilities of discovering so called 'hotspots,' which would arise if the gluon density is not spread uniformly over the hadron, but tends to build clusters. For a summary on 'hotspots' see [2, page 203 ff].

Low x events are characterized by a scattered electron in the backward (proton side) direction, where in a given angular region the electron energy basically determines x . By comparing the measured electron spectrum with a Monte Carlo simulating these effects, one should be able to distinguish between various models even at an integrated luminosity of 1 pb^{-1} [2, page 135].

Another area of interest is the photoproduction total cross section and hard scattering effects in the γp reaction. Various authors have extra-

polated the present data, which are available in a region of s below 200 GeV². At HERA this type of physics can be explored up to a center-of-mass energy of $s = 5 \times 10^4$ GeV². This can be studied with the present very low luminosity, and first results are given below.

Finally, as at all new accelerators, a search for exotic phenomena has already started. Obviously an ep collider is best suited to find any bound states the lepton-quark systems. However, searches for SUSY particles, leptogluons, and excited leptons, as well as pair production of new particles carrying new conserved quantum numbers, are also of great interest.

The physics possibilities of the HERA experiments are described in detail in [2].

3. The Experimental Challenge

3.1. The Detectors

The asymmetric nature of the ep collider is reflected in the fact that both detectors are much denser in the forward direction of the protons, where high energy jets are expected, and where the requirements of the energy and angular resolution are highest with respect to accurate determination of the event kinematics. Apart from this, both experiments consist of four main detector systems: tracking, calorimetry, main, and forward muon systems (see Figures 3.1 and 3.2).

Tracking: Both experiments have a tracking system around the interaction region, which is split into a central and a forward part. While the forward part in both experiments consists of a combination of various drift-chambers and transition radiators, the central tracker is significantly different: Zeus has chosen one big central drift chamber with stereo wire readout for measuring all three space coordinates and for use in complex triggering systems (to be implemented later). The H1 central tracker consists of a total of six concentric chambers, namely two big 'jet chambers' with slightly tilted drift cells to correct for the Lorentz angle, two z-chambers and two Multi Wire Proportional Chambers (MWPC). Triggering information is presently derived from the jet chamber and the MWPCs.

In the Zeus experiment the coil for the magnetic field is located just outside the tracker, while the H1 coil is mounted outside the calorimeter. Both coils are superconducting.

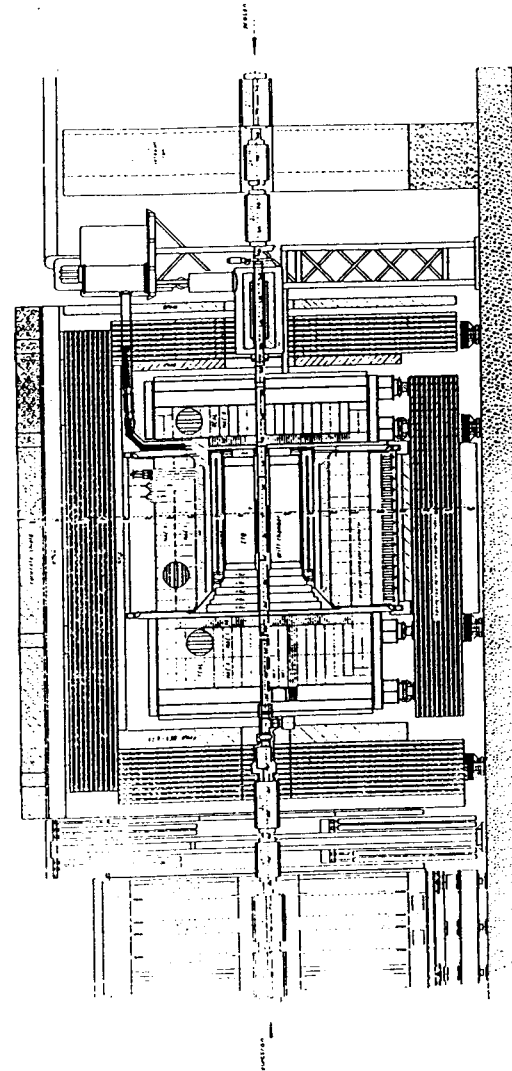


Figure 3.1: The Zeus detector. Protons enter from the right, electrons from the left.

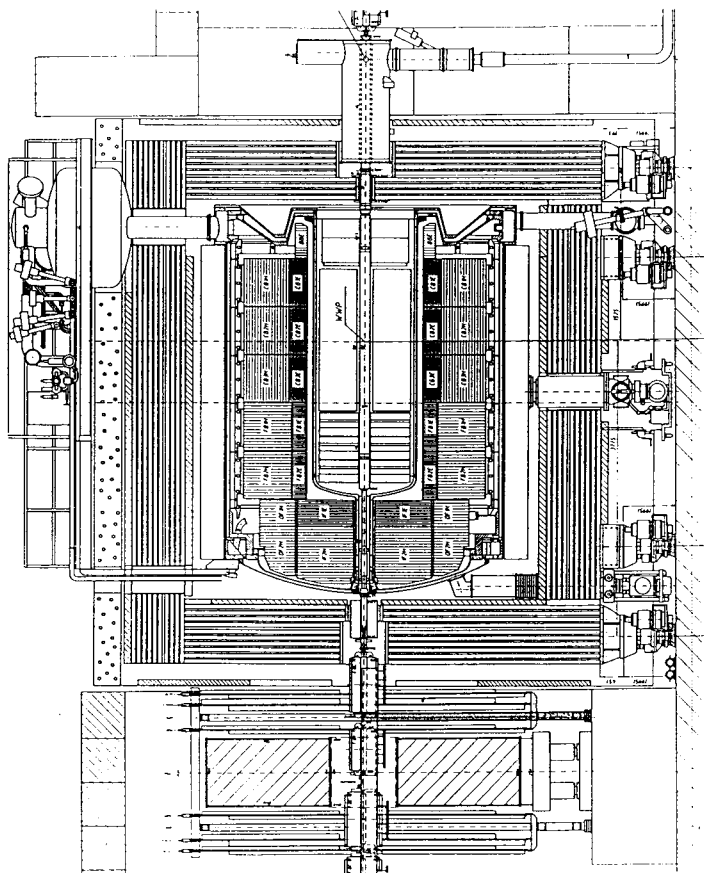


Figure 3.2: The H1 detector. Protons enter from the right, electrons from the left.

The Zeus calorimeter consists of a compensating depleted uranium - scintillator sandwich with wavelength shifter readout into some 13,000 photomultipliers. H1 has a liquid argon calorimeter with a total of 45,000 readout channels. The electromagnetic part consists of lead plates while the hadronic part is made of stainless steel plates. Compiling different responses for electromagnetic and hadronic interactions is achieved in H1 by a newly developed technique for weighting the signal from each individual pad. Resolution values have been determined by test beam measurements at CERN SPS and Monte Carlo studies, giving an electromagnetic (hadronic) resolution in Zeus of $18(35) \% / \sqrt{E}$ and in H1 of $12(45) \% / \sqrt{E}$ where a constant term of about 1% is to be added in all cases.

While the Zeus calorimeter covers the whole angular acceptance rather uniformly, H1 has a special warm lead scintillator sandwich backward calorimeter (BEMC) built in 88 stacks with corresponding transverse granularity of 16 by 16 cm². The readout is based on the signals of six photo-diodes per stack, and the expected resolution is $10\% / \sqrt{E} + 1\%$. In front of the BEMC, a flat MWPC allows determination of the exact entry point of particles into the BEMC.

Outside the calorimeter the magnetic field return yoke of both detectors is equipped with limited streamer tubes to detect single muons and leaking calorimetric showers. In addition, special muon boxes improve the identification and momentum measurement performance for muons.

3.2. Triggering and Data Acquisition Systems

At HERA, physics is seen through electroweak cross sections, while background is determined by the much bigger proton-nucleon cross sections. The most important backgrounds in these experiments are due to photons hitting the nuclei of the residual gas or hitting the beam tube walls. This presently gives a rate of a few hundred background events in the detector per second, which extrapolates to about 100 kHz at full luminosity. In contrast, any interesting physics processes happen only at rates below 1 Hz. Together with the bunch crossing interval of 96 ns, these poor signal-to-noise conditions mean that building and running trigger and data acquisition systems at HERA experiments are among the biggest challenges, to date in this field of particle physics.

Unfortunately, the signature of the background is not completely unique. Only events with most tracks not originating from the nominal interaction region are certainly not ep physics. Other indications for background involve combinations of selection criteria, among which are low total transverse energy, very forward (i.e. in p direction) oriented kinematics, many more positive than negative tracks or many protons in the final state.

The triggering and event filtering system consists of three levels in both experiments. In the first level, all detector signals and trigger decision paths are pipelined (length 2.5 to 5 microsec.), and the trigger decision is therefore taken completely free of dead time. Intermediate level triggers, able to kill the event readout, are foreseen but not used yet. Filter farms then process the full event data before the information is stored on cartridges. By the end of July more than 300 GByte (H1) of data had been stored in this way.

In the first level trigger both experiments presently use the total transverse energy in the calorimeter with position dependent thresholds, because background is much higher close to the beam pipe. H1 also makes use of an estimation of the vertex position along the beam axis, and cuts on timing information from a time of flight hodoscope in the proton's backward area. In both experiments the electron detector of the luminosity system allows triggering on selected photoproduction events.

In the filter farm Zeus does an extensive timing calculation, which relies on the very good timing resolution of their calorimeter and which allows determination of the primary vertex of the event along the beam axis under certain conditions of event topology. H1 recalibrates the calorimeter thresholds and does a full track and vertex reconstruction, thus allowing triggering on events with very low transverse energy, which would not exceed the minimum thresholds of the calorimeter.

Typical level 1 trigger rates presently are 20 Hz, while about eight events per second survive the filter farm cuts.

4. The First Data

4.1. Photoproduction Total Cross Section

The following preliminary analysis is taken as an example from H1. The data used correspond to an integrated luminosity of $994 \mu\text{b}^{-1}$ and were triggered by the electron detector as described above. The background rate of this trigger was much too high; consequently, a hit in the backward proportional chamber was required in addition. A statistical background subtraction, using the data from the above mentioned e pilot bunch leaves 602 ± 61 photoproduction events [1]. The acceptance of this trigger is dependent on assumptions about the relative contributions of the various subprocesses giving rise to the total photoproduction cross section. Varying these assumptions in a reasonable way shows, that this acceptance has a systematic uncertainty of 10% (further details can be found in [1]). Furthermore, the luminosity is measured to 10% accuracy, and the photon flux folded with the electron tagging acceptance is known to 8%. The resulting total cross section

$$\sigma_{\text{pp}^{\text{tot}}} = (150 \pm 15_{\text{stat}} \pm 19_{\text{syst}}) \mu\text{b}, \quad \langle E_{\text{pp}} \rangle = 192 \text{ GeV}$$

is shown in Figure 4.1 together with the measurements at low energies and some theoretical extrapolations. It compares well with the simplest model and excludes large values as predicted by the 'minijet' models [5].

4.2. Deep Inelastic Scattering

Figures 4.2 and 4.3 show candidates for deep inelastic scattering (DIS) events from both experiments. Because of the Q^{-4} dependence of the cross section, only events with low Q^2 , are expected with the present low statistics; however many events have in fact x values below 10^{-4} , which is two orders of magnitude less than presently available data from fixed target experiments.

Both experiments did an analysis of their DIS event sample; as an example, the results of H1 are explained here. They are based on an integrated luminosity of 1.5 nb^{-1} , for which an energy cluster in the backward calorimeter (BEMC) of more than 4 GeV in anticoincidence with the ToF hodoscope was required as a trigger. Further selection in the offline analysis required a reconstructed hit in the backward proportional chamber, a valid vertex determination from the charged tracks in the central jet chamber and the

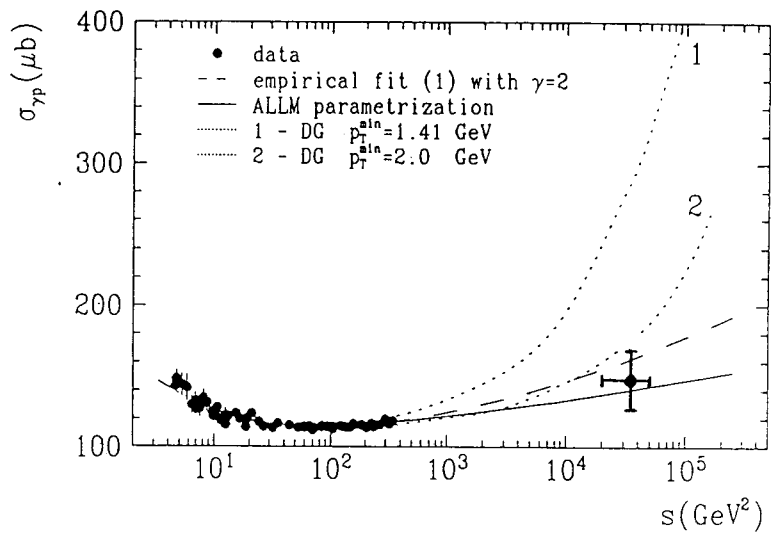


Figure 4.1.: The total photoproduction cross section as a function of the center-of-mass energy squared (s). The preliminary H1 result is shown (for explanation see text) together with old data and some theoretical extrapolations (references: ALLM [4], DG [5], empirical fit from S. Levonian in [2, page 499]).

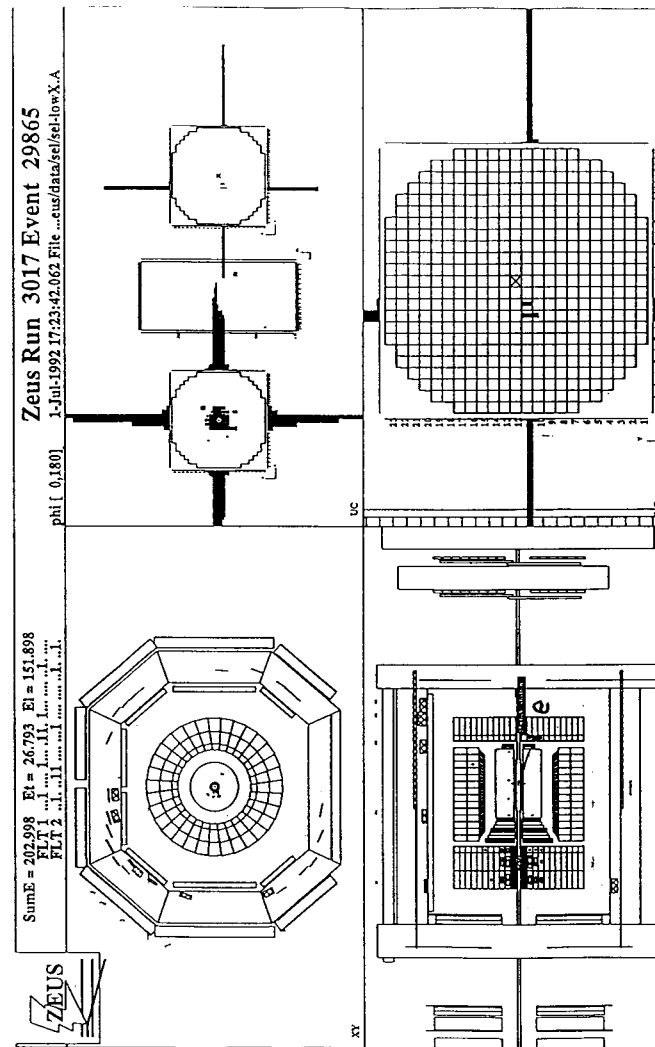


Figure 4.2: A deep inelastic neutral current event, seen by the Zeus detector.

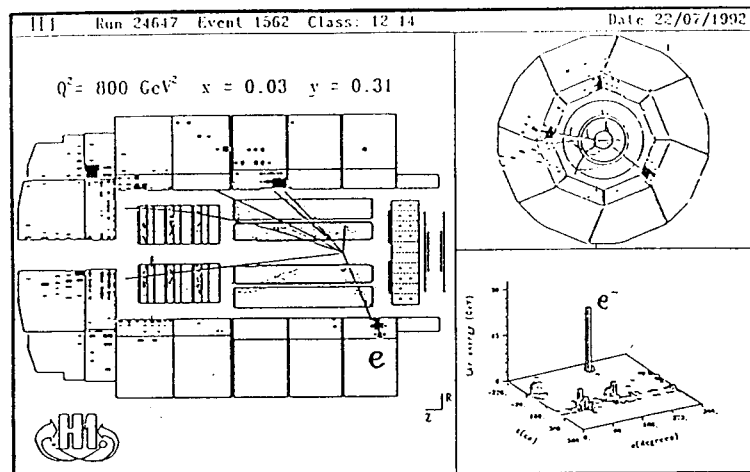


Figure 4.3: A deep inelastic neutral current event, seen by the H1 detector.

vertex to be within the nominal interaction region of ± 80 cm, unless the energy in the BEMC was higher than 22 GeV. Furthermore, some background events were rejected by visual scanning. Pilot bunch data showed that the contamination of proton background in the final sample of about 150 events is less than 10%.

The electron energy spectrum in Figure 4.4 (top) shows the expected significant peak at the beam energy of 26.7 GeV, which originates from the fact that for most of the phase space at low Q^2 , the energy loss of the electron (y) is very small. This so-called kinematic peak is very useful for checking the energy calibration of the calorimeters. The hashed area in the plot shows the Monte Carlo prediction of [3] absolutely normalised to the integrated luminosity on which the data are based. The flat region between 12 and 22 GeV is very sensitive to the various models for the transition regions mentioned previously, but as expected with the available limited statistics, no selection between such models can be made at present. Finally, below 12 GeV a contamination from pions originating from photo-production events can be seen, which in principle can be removed by the e/π separation capabilities of the BEMC or by kinematical selections on the hadronic final states; further analyses of these methods are in progress. Finally, the lower part of Figure 4.4 shows that the x and Q^2 distributions also agree well with the expectations from the Monte Carlo simulation.

5. Outlook

HERA operated this summer with 0.2% of its design luminosity due to reduced beam currents and the small number of filled bunches. No major difficulties in increasing the performance step-wise to the design values in the near future are expected. But it is still a major challenge to the experimental collaborations to improve the performance of their detectors, especially in the areas of trigger and event filtering systems, in order to cope with the higher beam intensities anticipated.

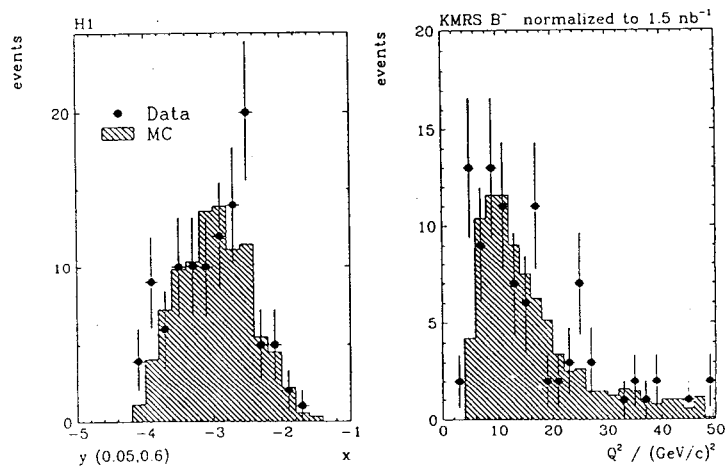
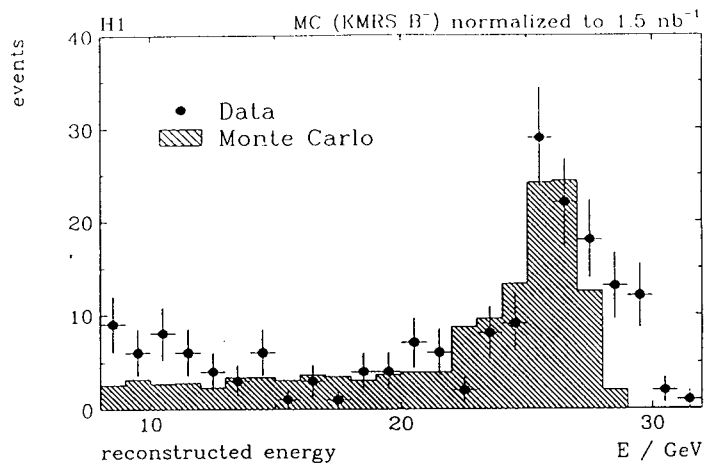


Figure 4.4: Reconstructed quantities of the neutral current event sample of H1: energy of the scattered electron (top), x (bottom left) and Q^2 (bottom right). The hashed histogram corresponds to Monte Carlo simulation, based on the model in [3].

References:

- [1] F. Eisele: First Results from the H1 Experiment at HERA, Proceedings of the International Conference on High Energy Physics, Dallas 1992.
- [2] Physics at HERA, edited by W. Buchmueller and G. Ingelmann, Proceedings of the HERA Workshop, Hamburg 1992.
- [3] J. Kwiecinsky, A.D. Martin, W.J. Stirling and R.G. Roberts, Phys. Rev. D42, 3645 (1990).
- [4] H. Abramowicz et al., Phys. Lett. B269, 465 (1991).
- [5] M. Drees and K. Grassie, Z. Phys. C28, 451 (1985).